International Journal of Bifurcation and Chaos

Loss of determinacy at small scales, with application to multiple time-scale and nonsmooth dynamics

S. Webber, M. R. Jeffrey
Dept. of Engineering Mathematics, University of Bristol, Bristol BS8 1UB, UK, email: mike.jeffrey@bristol.ac.uk

A singularity is described that creates a forward time loss of determinacy in a two-timescale system, in the limit where the timescale separation is large. We describe how the situation can arise in a dynamical system of two fast variables and three slow variables or parameters, with weakly coupling between the fast variables. A wide set of initial conditions enters the ε-neighbourhood of the singularity, and explodes back out of it to fill a large region of phase space, all in finite time. The scenario has particular significance in application to piecewise-smooth systems, where it arises in the blow up of dynamics at a discontinuity and is followed by abrupt re-collapse of solutions to 'hide' the loss of determinacy, and yet leave behind a remnant of it in the global dynamics. This constitutes a generalization of a 'micro-slip' phenomenon found recently in spring-coupled blocks, whereby coupled oscillators undergo unpredictable stick-slip-stick sequences instigated by a higher codimension form of the singularity. The indeterminacy is localised to brief slips events, but remains evident in the indeterminate sequencing of near-simultaneous slips of multiple blocks.

Keywords: discontinuity, sliding, sticking, friction, slip, switching, oscillators

1. Introduction

The determinacy of a dynamical system — the property that the system defines unique behaviour from a given initial state — requires it to be differentiable at any point. This means that indeterminacy is commonplace in *piecewise-smooth* (or more simply *nonsmooth*) systems, which suffer loss of continuity along isolated thresholds in space that represent things like collisions [Stewart, 2000; Stronge, 2004; Jiang et al., 2017], frictional stick-slip [Hinrichs et al., 1998; Wojewoda et al., 2008; Kowalczyk & Piiroinen, 2008], electronic switching [di Bernardo et al., 1998; Shi et al., 1999; Wang et al., 2017]. Outside these traditional applications are a growing number of others such as genetic regulation [Davidson & Levin, 2005; Casey et al., 2006; Acary et al., 2014; Karlebach & Shamir, 2008; Plahte & Kjøglum, 2005], and abrupt transitions in climate modeling [Barry et al., 2014; Leifeld, 2016; Roberts & Glendinning, 2014].

There are a number of basic ways that determinacy can be lost in a nonsmooth system, and we can describe them with a few simple toy models. The simplest is illustrated by the point $x = 0$ in the system $\dot{x} = \sqrt{|x|}$ or $\dot{x} = 2 + x/|x|$, which can be shown to admit an infinity of different solutions that each pause for a different time as they *cross* through the discontinuity [Glendinning et al., 2019]. After this, perhaps the most important behaviour of nonsmooth systems is called *sliding* or *sticking*, in which solutions collapse in finite time onto a discontinuity, as in a system $\dot{x} = -x/|x|$, $\dot{y} = 1$, where solutions all collapse onto the constrained state $x = 0$. Switches much like these are commonplace in models of control and regulatory switching in electronics, mechanics, and physiology. The converse to the last example is a

system $\dot{x} = x/|x|$, where any point on $x = 0$ explodes into an infinity of distinct trajectories that may stick to $x = 0$ for arbitrary times before departing along the real line. Figure 1 illustrates sticking, explosion, and a combination of the two giving arbitrary pausing during crossing, at a discontinuity surface (shown in 2 dimensions).

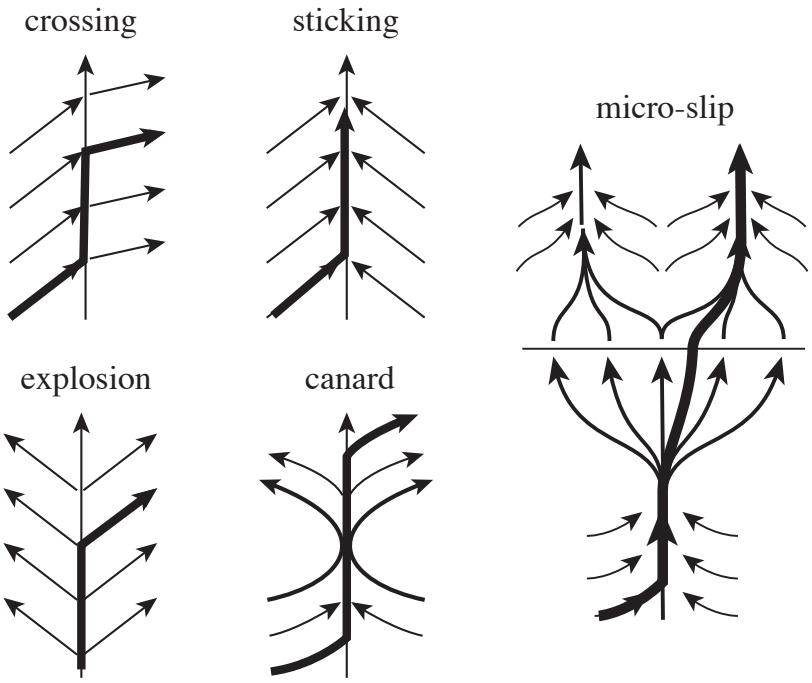

Fig. 1. Basic mechanisms of indeterminacy in nonsmooth system. For the simple mechanisms of sticking, explosions, crossing, and canards, we sketch the toy models described in the text $\dot{x} = ...x/|x|...$, along with $\dot{y} = 1$ for illustration. For micro-slip we show a schematic of the scenario studied in this paper (the scenario in [Webber & Jeffrey, 2019] re-collapses to one outgoing trajectory instead of two). For each example one of the many possible solutions is shown bold.

Examples like these are sometimes used in courses on differential equations to illustrate poorly defined systems, and yet they do arise in applications, so it is necessary to ask how to analyze and interpret them when they do arise, in particular what implications their indeterminacy has for a system's behaviour.

The indeterminable exit of states caricatured by the examples above become interesting in applications because there exist so-called *canard* trajectories that can travel from attracting to repelling regions of a discontinuity threshold, from collapsing behaviour like $\dot{x} = -x/|x|$ to explosive behaviour like $\dot{x} = -x/|x|$, as the solution $x(t) = 0$, $y(t) = t$, does in the system $\dot{x} = yx/|x|$, $\dot{y} = 1$. An example of a canard in a nonsmooth system is shown in fig. 1.

A new mechanism of indeterminacy was discovered more recently in [Webber & Jeffrey, 2019] in the context of coupled dry-friction oscillators. The phenomenon is a localised loss of determinism that is rapidly followed by re-collapse to deterministic evolution. In the mechanical oscillator this manifests as micro-slip of the coupled oscillators, a small 'shuffling' of the oscillators in an interminable ordering prior to the ensuing of macroscopic slip. The effect is highly localized, and yet the brief loss of determinism can have global effects, both in the macroscopic motions of the oscillators and the forces they experience.

The singularity underlying the indeterminacy described in [Webber & Jeffrey, 2019] is somewhat degenerate, owing to the lack of coupling between the frictional forces between simple mechanical oscillators. Here we show the form the phenomenon might take in wider applications by deriving a more general local form for the singularity, specifically one that permits weak coupling between the main system variables (in the context of [Webber & Jeffrey, 2019] this would constitute a weak coupling between the frictional contact forces). Although an initial loss of determinacy at the singularity is followed by a re-collapse of solutions, the collapse may fall onto different trajectories that give distinct global outcomes, illustrated schematically by the 'micro-slip' picture in fig. 1.

Consider planar variables $(\eta_1, \eta_2) \in \mathbb{R}^2$, evolving according to a system

$$\varepsilon_1 \dot{\eta}_1 = g_1(\eta_1, \eta_2) \ , \tag{1}$$
$$\varepsilon_2 \dot{\eta}_2 = g_2(\eta_1, \eta_2) \ , \tag{2}$$

where $\varepsilon_1, \varepsilon_2$, are small positive constants, and g_1, g_2, are smooth functions.

The singularity of interest is a point $(\eta_1, \eta_2) = (0, 0)$ that satisfies the conditions

$$g_i(0,0) = \frac{\partial}{\partial \eta_i} g_i(0,0) = 0 \neq \frac{\partial^2}{\partial \eta_i^2} g_i(0,0) \ , \qquad i = 1, 2, \tag{3}$$

with either no coupling (as considered in [Webber & Jeffrey, 2019]),

$$g_i(\eta_1, \eta_2) = g_i(\eta_i) \ , \qquad i = 1, 2, \tag{4}$$

or weak coupling defined as

$$0 = \frac{\partial}{\partial \eta_2} g_1(0,0) \ , \tag{5a}$$
$$\frac{\partial^2}{\partial \eta_i^2} g_i(0,0) \gg \frac{\partial^2}{\partial \eta_j^2} g_i(0,0) \ , \qquad i \neq j \in \{1, 2\}. \tag{5b}$$

The conditions (3) define an equilibrium of the $(\dot{\eta}_1, \dot{\eta}_2)$ system undergoing a form of degenerate fold bifurcation. In the uncoupled system defined by (4) this occurs as a two-parameter bifurcation. It was in this context that the singularity was found in the stick-slip behaviour of a pair of frictional oscillators in [Webber & Jeffrey, 2019], in which the two parameters needed to unfold the bifurcation are provided by the states of the oscillators. If coupling is allowed then this instead constitutes a codimension four singularity, but if we impose the weaker conditions (5) giving weak coupling, a codimension three singularity provides similar behaviour which, despite being less degenerate, produces more extreme global consequences. We shall study both cases here.

The right-hand side may also depend on the constants $\varepsilon_1, \varepsilon_2$, but we need not make this explicit. The significance of $\varepsilon_1, \varepsilon_2$, is in providing fast timescales for the dynamics of (η_1, η_2) in a system with slow variables x_1 and x_2, say as $\dot{x}_1 = f_1(x_1, x_2, \eta_1, \eta_2)$ and $\dot{x}_2 = f_2(x_1, x_2, \eta_1, \eta_2)$, which we will explore in application to multiple timescale or piecewise-smooth systems in section 3-section 5 below.

We derive a local form for the singularity in section 2. The higher codimension form of the singularity is studied in section 3, providing a brief summary of the study from [Webber & Jeffrey, 2019], before going on to study the more general lower codimension case in section 4. In each section the singularity is studied first in the planar (η_1, η_2) system, and then this is considered as the fast planar part of a two timescale system. The application to piecewise-smooth dynamics is considered in section 5, where the singularity arises when blowing up or regularizing a discontinuity. Some concluding remarks are made in section 6.

2. A normal form

Let us first derive a local expression for a singularity satisfying (3)-(5). Consider $\eta_j \in V$ and $0 \leq \varepsilon_j \ll 1$ for $j = 1, 2$, where V is an open set such that $0 \in V$. Expand (1) for small η_1, η_2, as

$$\varepsilon_1 \dot{\eta}_1 = a_0 - a_1\eta_1 - a_2\eta_2 - a_3\eta_1^2 - a_4\eta_1\eta_2 - a_5\eta_2^2 + \mathcal{O}\left(|\eta_1, \eta_2|^3\right) \ , \tag{6a}$$
$$\varepsilon_2 \dot{\eta}_2 = b_0 - b_1\eta_1 - b_2\eta_2 - b_3\eta_1^2 - b_4\eta_1\eta_2 - b_5\eta_2^2 + \mathcal{O}\left(|\eta_1, \eta_2|^3\right) \ , \tag{6b}$$

about the origin. This assumes that g_1 and g_2 are at least three times differentiable in η_1 and η_2. Any $\varepsilon_1, \varepsilon_2$, dependence is taken inside the coefficients a_i, b_i, which may therefore be considered as $a_i + \mathcal{O}(\varepsilon_1, \varepsilon_2)$ and $b_i + \mathcal{O}(\varepsilon_1, \varepsilon_2)$, without qualitatively altering the results below. Let us then try to simplify these by reducing to only those terms needed explicitly to satisfy the conditions (3).

By a simple linear transformation we can eliminate the bilinear $\eta_1\eta_2$ term in each row of (6). The non-degeneracy conditions (i.e. the inequalities) in (5) imply $a_3, b_5 \neq 0$, and these can be scaled to $a_3 =$

$b_5 = 1$. A simple translation places the point satisfying the conditions (3) at the origin (effectively setting $a_1 = b_2 = 0$). Applying the weak coupling conditions (5), we have $a_2 = 0$ and (6) becomes

$$\varepsilon_1 \dot{\eta}_1 = a_0 - \eta_1^2 + \mathcal{O}\left(\eta_2^3, \eta_1^2, \eta_1\eta_2^2\right) , \tag{7a}$$

$$\varepsilon_2 \dot{\eta}_2 = b_0 - b_1\eta_1 - \eta_2^2 + \mathcal{O}\left(\eta_1^3, \eta_2^2, \eta_1^2\eta_2\right) . \tag{7b}$$

Thus we have three parameters, a_0, b_0, b_1, and when these vanish the codimension three singularity defined by (3) occurs at the origin. In an un-coupled system described by (4), b_1 vanishes and the singularity has codimension two.

We will study the truncation of (7) that omits the higher order terms.

We consider only the case where ε_1 and ε_2 are of a similar order, so that

$$\lim_{\varepsilon_1,\varepsilon_2\to 0} \frac{\varepsilon_1}{\varepsilon_2} = L \neq 0 \tag{8}$$

for some finite L. For simplicity we therefore take $\varepsilon_1 = \varepsilon_2$, without loss of generality, the more general case requiring only inserting a further constant L throughout the analysis if, for example, $\varepsilon = \varepsilon_1 = L\varepsilon_2$.

The non-vanishing of the second derivatives in (3) prevent higher order degeneracy of the singularity. The conditions in (5) imbue the singularity with the local character of interest to us here, namely the conditions for indeterminacy. Replacing the '$\gg$' symbol in (5b) directly with a '$\ll$' symbol (i.e. strong nonlinear coupling) yields a fully deterministic case, and a more complete study of the singularity might consider the full range of behaviours, but for brevity we restrict ourselves to the case given by (3), making only a few more general remarks in section 6.

3. Uncoupled case and oscillator

We first study the planar (η_1, η_2) singularity when $a_0 = b_0 = 0$, before looking at its significance as the fast subsystem of a two-timescale problem with a_0 and b_0 replaced by slow variables.

If we set $a_0 = b_0 = 0$ in (7) and truncate the expansion to remove higher order terms, and assume an uncoupled system (implying $b_1 = 0$ by (4)), we obtain

$$\varepsilon\dot{\eta}_1 = -\eta_1^2 , \tag{9a}$$

$$\varepsilon\dot{\eta}_2 = -\eta_2^2 . \tag{9b}$$

Clearly this consists of a pair of one-dimensional systems undergoing a saddle-node bifurcation (or fold catastrophe), so there is little new of interest to be discovered about the system itself, but it will become of interest when coupled with slower (ε independent) dynamics. To this end we will first show that there exist a set of orbits of (9) that exit the ε-neighbourhood of the origin in finite time, creating set-valued exit from the singularity as $\varepsilon \to 0$.

Lemma 1. *The flow of* (9) *exits the ε-neighbourhood of the singularity at $(\eta_1, \eta_2) = (0, 0)$ in finite time, and in doing so fills the region $\eta_1, \eta_2 < 0$.*

Proof. Solutions of (9) are given by

$$\eta_1(t) = \frac{\eta_1(0)}{1 + \eta_1(0)\frac{t}{\varepsilon}} , \qquad \eta_2(t) = \frac{\eta_2(0)}{1 + \eta_2(0)\frac{t}{\varepsilon}} , \tag{10}$$

and these lie on curves expressible as

$$\eta_2(t) = \frac{\eta_1(t)}{1 - C\eta_1(t)} , \tag{11}$$

for $C = \frac{1}{\eta_1(0)} - \frac{1}{\eta_2(0)} \in \mathbb{R}$. These are plotted in fig. 2. For every $C \in \mathbb{R}$ there exists a different curve (11) passing through the singularity $(\eta_1, \eta_2) = (0, 0)$, hence there are an infinite number of such solutions. Letting $C \to \pm\infty$ we obtain the outermost solutions of the set, lying along the half lines $\eta_1(0) = 0 > \eta_2$ and $\eta_2 = 0 > \eta_1$, and thus (11) defines a continuum of curves filling the region $\eta_1, \eta_2 < 0$ bounded by these half-lines.

The time taken by the solutions (10) to escape from an ε-neighbourhood of origin, say from $\eta_1 = -\varepsilon$ to $\eta_1(T) \ll -\varepsilon$, is then given by solving

$$\eta_1(T) = \frac{\eta_1(0)}{1+\eta_1(0)\frac{T}{\varepsilon}} \qquad \Rightarrow \qquad T = 1 + \frac{\varepsilon}{\eta_1(T)} \,, \tag{12}$$

hence they exit the ε-neighbourhood of the singularity in a time $T \sim 1 + \mathcal{O}(\varepsilon)$.

■

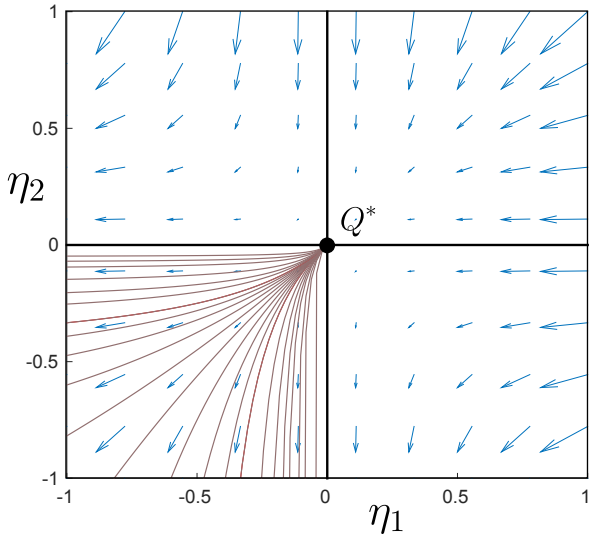

Fig. 2. The flow of (9), showing how solutions exit the ε-neighbourhood of the singularity (at Q^*) to fill the region $\eta_1, \eta_2 < 0$ in finite time.

The singularity is, of course, merely a simultaneous fold catastrophe in each of the un-coupled one-dimensional systems in η_1 and η_2, and without the small ε would not be of much interest. The significance is only realised in the context of a system where (9) represents the fast subsystem of a higher dimensional two-timescale system. The singularity then lies on the critical manifold $\eta_1 = \eta_2 = 0$ in the space of the full system. It is then possible for a the slow-fast dynamics to exponentially contract solutions into the neighbourhood of the singularity in finite time, and from there for them to exit in finite time, 'exploding' outward to fill the entire plane quadrant $\eta_1, \eta_2 \leq 0$.

To illustrate this consider the system

$$\dot{x}_1 = v_1 + \mathcal{O}(\varepsilon) \,, \tag{13a}$$
$$\dot{x}_2 = v_2 + \mathcal{O}(\varepsilon) \,, \tag{13b}$$
$$\varepsilon\dot{\eta}_1 = -x_1 - \eta_1^2 \,, \tag{13c}$$
$$\varepsilon\dot{\eta}_2 = -x_2 - \eta_2^2 \,, \tag{13d}$$

which is a toy model of the singularity from [Webber & Jeffrey, 2019] (more precisely, the oscillator studied in [Webber & Jeffrey, 2019] can be placed in this form local to the singularity by a suitable change of x_i-coordinates). In short, a one-parameter family of solutions are attracted into an exponentially small (in ε) neighbourhood of the singularity in finite time, and from there repelled to fill the region $\eta_1, \eta_2 < 0$ in finite time, making them indistinguishable in an ε-neighbourhood of the singularity. We show this more formally as follows. For brevity we shall neglect the $\mathcal{O}(\varepsilon)$ term in the slow subsystem (13a)-(13b).

Exponential contraction to the singularity in finite time is shown by the following.

Lemma 2. *A one-parameter family of orbits are attracted in finite time into a neighbourhood of the singularity in* (13) *that is exponentially small in* ε.

Proof. The points where the fast subsystem (9b) vanishes define a two-dimensional critical manifold of (13), given by

$$\mathcal{M} = \left\{(x_1, x_2, y_1, y_2) \in U^2 \times V^2 \ : \ x_1 = -\eta_1^2,\ x_2 = -\eta_2^2\right\} \ , \tag{14}$$

which has an attracting branch in $\eta_1, \eta_2 > 0$ and repelling branch in $\eta_1, \eta_2 < 0$. For $\varepsilon = 0$ this defines an invariant set of (13). For $\varepsilon > 0$, by the theory of Fenichel [Fenichel, 1979; Jones, 1995], there exist invariant manifolds $\mathcal{M}_\varepsilon$ in an ε-neighbourhood of $\mathcal{M}$ away from $\eta_1 = \eta_2 = 0$ (at which $\mathcal{M}$ loses normal hyperbolicity).

Trajectories away from $\mathcal{M}$ are attracted to an ε-neighbourhood $\mathcal{M}$ in a time $t = \mathcal{O}(\varepsilon)$, and moreover contract exponentially as they approach $\mathcal{M}_\varepsilon$. Take an initial condition $(x_1, x_2, \eta_1, \eta_2) = (-\xi_1, -\xi_2, \sqrt{\xi}_1 + z_1, -\sqrt{\xi}_2 + z_2)$ with $p, q > 0$. The fast equations (13c)-(13d) give $\varepsilon \dot{z}_i = \xi_i - v_i t - (\sqrt{\xi}_i + z_i)^2 = -v_i t - 2 z_i \sqrt{\xi}_i + \mathcal{O}\left(z_i^2\right)$ for $i = 1, 2$, with solution

$$z_i(t) = \frac{\varepsilon v_i}{4\xi_i} - \frac{v_i t}{2\sqrt{\xi}_i} + \left(z_i(0) - \frac{\varepsilon v_i}{4\xi_i}\right) e^{-2\sqrt{\xi}_i t/\varepsilon} \ . \tag{15}$$

This shows firstly that in a time $t = \mathcal{O}(\varepsilon)$ a solution will approach exponentially close to $z_i(t) = \frac{\varepsilon v_i}{4\xi_i} - \frac{v_i t}{2\sqrt{\xi}_i}$, which must lie on some invariant manifold $\mathcal{M}_\varepsilon$ close to $\mathcal{M}$. Moreover, any two such solutions with different initial conditions $z_i(0)$ and $\hat{z}_i(0)$, but the same x_i, contract to a separation of $\mathcal{O}\left(e^{-2\sqrt{\xi}_i t/\varepsilon}\right)$ as t increases. If the solutions are also separated in x_i space, with different initial conditions ξ_i and $\hat{\xi}_i$, they also contract, but to a separation of

$$\begin{aligned} z_i(t) - \hat{z}_i(t) &= \tfrac{1}{4}\varepsilon v_i(\tfrac{1}{\xi}_i - \tfrac{1}{\hat{\xi}_i}) - \tfrac{1}{2} v_i t(\tfrac{1}{\sqrt{\xi}_i} - \tfrac{1}{\sqrt{\hat{\xi}_i}}) + \mathcal{O}\left(e^{-2\sqrt{\xi}_i t/\varepsilon}\right) \\ &= -\tfrac{\varepsilon v_i \xi_i}{4X_i^2} - \tfrac{v_i t \xi_i}{4X_i^{3/2}} + \mathcal{O}\left(e^{-2\sqrt{\xi}_i t/\varepsilon}\right) \end{aligned} \tag{16}$$

expanding for large $X_i = \hat{\xi}_i - \xi_i$, that is, an inverse 3/2 power of their initial separation.

Having contracted exponentially towards a manifold $\mathcal{M}_\varepsilon$, again by Fenichel's theory, the dynamics on $\mathcal{M}_\varepsilon$ is an ε-perturbation of (9a) with $\dot{\eta}_1 = \dot{\eta}_2 = 0$. Taking again $\xi_1, \xi_2 > 0$, and initial conditions on $\mathcal{M}$ given by

$$(x_1(0), x_2(0), \eta_1(0), \eta_2(0)) = \left(-\xi_1, -\xi_2, -\xi_1^2, -\xi_2^2\right) \ , \tag{17}$$

let us fix $\xi_2 = \xi_1 v_2 / v_1$. The solution through this point, namely

$$\begin{aligned} (x_1(t), x_2(t), \eta_1(t), \eta_2(t)) = \big(&v_1 t - \xi_1, v_2 t - \xi_2, \\ &- (v_1 t - \xi_1)^2, -(v_2 t - \xi_2)^2\big) \ , \end{aligned} \tag{18}$$

evolves in time $t = \xi_1 / v_1$ to the singularity, that is to

$$(x_1(\xi_1/v_1), x_2(\xi_1/v_1), \eta_1(\xi_1/v_1), \eta_2(\xi_1/v_1)) = (0, 0, 0, 0) \ . \tag{19}$$

As we showed, there exist a one-parameter (ξ_1) family of trajectories that contract exponentially towards such an orbit, and therefore arrive within an exponentially small neighbourhood of the singularity in this time (and further orbits separated in x_i space which contract to an inverse 3/2 power of their initial separation of such a trajectory).

■

Exit from the neighbourhood of singularity occurs in finite time, exploding to fill the region $\eta_1, \eta_2 < 0$, as is shown by the following.

Lemma 3. *Orbits with initial conditions in an* ε*-neighbourhood of the singularity in the region* $\eta_1, \eta_2 < 0$*, lie an order 1 distance from the singularity after a time* $t = \mathcal{O}\left(\varepsilon^{2/3}\right)$.

Proof.

To consider how solutions exit the singularity, we can first write the solutions to the full system (13) as

$$x_i(t) = -\xi_i + v_i t + \mathcal{O}(\varepsilon) \ , \tag{20a}$$

$$\eta_i(t) = -(\varepsilon v_i)^{1/3} \frac{Bi'(s_i) + c_i Ai'(s_i)}{Bi(s_i) + c_i Ai(s_i)} \ , \tag{20b}$$

where, letting $\eta_i(0) = \eta_{i0}$,

$$s_i = -\frac{t v_i^{1/3}}{\varepsilon^{2/3}} \ , \qquad c_i = \sqrt{3} \frac{\frac{(2/3)!}{(1/3)!}(3\varepsilon v_i)^{1/3} + \eta_{i0}}{\frac{(2/3)!}{(1/3)!}(3\varepsilon v_i)^{1/3} - \eta_{i0}} \ . \tag{21}$$

For $t \ll \varepsilon^{2/3}/v_i^{1/3}$ (small s_i) we can expand this as

$$x_i(t) = -\xi_i + v_i t + \mathcal{O}(\varepsilon) \ , \tag{22a}$$

$$\begin{aligned} \eta_i(t) &= -(\varepsilon v_i)^{1/3} \frac{[\frac{3^{1/6}}{(\frac{1}{3})!} + \frac{s^2}{2.3^{1/6}(\frac{2}{3})!}] + c_i[-\frac{1}{3^{1/3}(\frac{1}{3})!} + \frac{s^2}{2.3^{2/3}(\frac{2}{3})!}]}{[\frac{3^{1/6}s}{(\frac{1}{3})!} + \frac{1}{3^{1/6}(\frac{2}{3})!}] + c_i[-\frac{s}{3^{1/3}(\frac{1}{3})!} + \frac{1}{3^{2/3}(\frac{2}{3})!}]} + \mathcal{O}\left(\varepsilon^{1/3}s^3\right) \\ &= -(\varepsilon v_i)^{1/3} \frac{d_i + \frac{1}{2}s_i^2}{1 + d_i s_i} + \mathcal{O}\left(\varepsilon^{1/3}s^3\right) \ , \quad d_i = \frac{3^{1/3}(2/3)!(1 - \frac{c_i}{\sqrt{3}})}{(1/3)!(1 + \frac{c_i}{\sqrt{3}})} \ . \end{aligned} \tag{22b}$$

Note there exists an orbit that passes through the singularity, given by letting $\eta_{i0} = 0$, which gives $c_i = \sqrt{3}$ above, and leaves us with

$$x_i(t) = -\xi_i + v_i t + \mathcal{O}(\varepsilon) \ , \tag{23a}$$

$$\eta_i(t) = -\frac{v_i t^2}{2\varepsilon} + \mathcal{O}\left(\varepsilon^0\right) \ , \tag{23b}$$

so in a time $t = \mathcal{O}(\sqrt{\varepsilon})$ this solution passes escapes to an order one distance from the singularity. We are interested, however, in orbits that begin close to this near the singularity.

Let us find the time taken to reach or escape from an initial coordinate $\eta_{i0} < 0$ in the ε-neighbourhood of the singularity, that is $\eta_{i0} = \mathcal{O}(\varepsilon)$. Expanding (21) for small η_{i0} we have

$$c_i = \sqrt{3}\left(1 + 2\frac{\eta_{i0}}{\frac{(2/3)!}{(1/3)!}(3\varepsilon v_i)^{1/3}}\right) + \mathcal{O}\left((\eta_{i0}/\varepsilon^{1/3})^2\right) \ , \tag{24}$$

which in (22) (i.e. assuming $t = \mathcal{O}(\varepsilon)$) gives $d = -\frac{\eta_{i0}}{(\varepsilon v_i)^{1/3}} + \mathcal{O}\left((\eta_{i0}/\varepsilon^{1/3})^2\right)$, and hence

$$x_i(t) = -\xi_i + v_i t + \mathcal{O}(\varepsilon) \ , \tag{25a}$$

$$\begin{aligned} \eta_i(t) &= -(\varepsilon v_i)^{1/3}\left(d + \tfrac{1}{2}s^2\right)(1 - ds) + \mathcal{O}\left(d^2,\ \varepsilon^{1/3}s^3\right) \\ &= \left(\eta_{i0} + \frac{t^2 v_i}{2\varepsilon}\right) + \mathcal{O}\left(\eta_{i0}^2/\varepsilon^{1/3},\ \varepsilon\right) \ , \end{aligned} \tag{25b}$$

which is also of order ε (recalling that we have assumed here the orders $t \sim \eta_{i0} \sim \varepsilon$).

Now, the solutions $\eta_i(t)$ as given by (20) exhibit finite time blow-up. We can locate this using the large s_i asymptotics (even though s_i will turn out to be of zero order in ε). Expanding (11) for large negative s_i

gives

$$x_i(t) = -\xi_i + v_i t + \mathcal{O}(\varepsilon) \ , \tag{26a}$$

$$\begin{aligned}\eta_i(t) &= (\varepsilon v_i)^{1/3}\sqrt{-s_i}\,\frac{\mathcal{T}_i - \frac{7}{48}(-s_i)^{-3/2}}{1-\frac{5}{48}(-s_i)^{-3/2}\mathcal{T}_i} \\ &= \frac{\frac{3}{2}\varepsilon\sqrt{t_*}}{t^{3/2}-t_*^{3/2}} + \mathcal{O}\left(\mathcal{C}_i^2, \tfrac{1}{\varepsilon}(t^{3/2}-t_*^{3/2})^0\right) \\ &= \frac{\varepsilon}{t-t_*} + \mathcal{O}\left(\varepsilon(t-t_s)^0, \varepsilon^2\right)\end{aligned} \tag{26b}$$

where

$$\mathcal{T}_i = \tan(\theta_i - \tfrac{\pi}{4} - \tfrac{2}{3}(-s_i)^{3/2}) \tag{27}$$

$$\theta_i = \arctan c_i \tag{28}$$

and

$$\mathcal{C}_i = \cot(\theta_i - \tfrac{\pi}{4} - \tfrac{2}{3}(-s_{i*})^{3/2}) = \tfrac{5}{48}(-s_{i*})^{-3/2} \ . \tag{29}$$

Thus in a time $t = t_* + \mathcal{O}(\varepsilon)$ a solution reaches an order 1 distance from the singularity. (We note the expansion above is valid with the 'large s_i' asymptotics being essentially for large s_{i*} or t_*). The time t_* is found by considering that, from (29), s_{i*} is the solution of a transcendental equation independent of ε, so s_{i*} is order one, implying $t_* \sim -\varepsilon^{2/3}s_{i*} = \mathcal{O}\left(\varepsilon^{2/3}\right)$, or $t = t_* + \mathcal{O}(\varepsilon) = \mathcal{O}\left(\varepsilon^{2/3}\right) + \mathcal{O}(\varepsilon)$.

■

Thus a combination of slow and fast dynamics bring a one-parameter family of orbits to the ε-neighbourhood of the singularity in finite time, from which they explode outward in $\varepsilon^{2/3}$ time, giving indeterminacy in the limit $\varepsilon \to 0$.

In section 5 we will go a step further and embed this slow-fast system inside the switching layer of a piecewise-smooth system, similar to the context it first arose in [Webber & Jeffrey, 2019], which constitutes a class of systems where $\varepsilon = 0$ exactly.

4. Weakly coupled case

Similar to the previous section, here we first study the planar (η_1, η_2) singularity when $a_0 = b_0 = 0$, before moving on to its role in a two-timescale problem with a_0 and b_0 replaced by slow variables.

Setting $a_0 = b_0 = 0 \neq b_1$ in (7) and truncating to omit the higher order terms, we have

$$\varepsilon\dot{\eta}_1 = -\eta_1^2 \ , \tag{30a}$$

$$\varepsilon\dot{\eta}_2 = -b_1\eta_1 - \eta_2^2 \ , \tag{30b}$$

in which the η_1-η_2 equations are weakly coupled. Although this is less degenerate than (9), a similar singularity persists, and as we shall see, this in fact has more extreme global consequences than we saw in section 3.

We begin by establishing, similarly to the previous section, that there exist a set of orbits of (30) that exit the ε-neighbourhood of the origin in finite time, creating set-valued exit from the singularity as $\varepsilon \to 0$.

Lemma 4. *The flow of* (30) *exits the ε-neighbourhood of the singularity at $(\eta_1, \eta_2) = (0, 0)$ in finite time, and in doing so fills the region $\eta_2 \leq \eta_2^{0,\infty}(\eta_1) \leq 0$, where $\eta_2^{0,\infty}(\eta_1)$ is a function to be defined.*

Proof. The equation (30a) for the dynamics of η_1 is the same as that of the uncoupled system (9a), with solution

$$\eta_1(t) = \frac{\eta_1(0)}{1+\eta_1(0)\frac{t}{\varepsilon}} \ . \tag{31}$$

Thus the finite time escape from an ε-neighbourhood of the singularity follows by lemma 1. It remains to show what region of the plane is filled by the flow from this neighbourhood.

Solutions for η_2 can be found in terms of η_1 by solving

$$\frac{d\eta_2}{d\eta_1} = \frac{\dot\eta_2}{\dot\eta_1} = \frac{b_1\eta_1 + \eta_2^2}{\eta_1^2} \ . \tag{32}$$

For $\eta_1 > 0$ the solution is best written in terms of Bessel functions,

$$\eta_2 = \frac{\eta_1}{2}\left(1 + \frac{w}{2}\frac{Y_2(w) - Y_0(w) - cJ_2(w) + cJ_0(w)}{cJ_1(w) - Y_1(w)}\right) \ , \tag{33}$$

where $w = 2\sqrt{b_1/\eta_1}$ and $c \in \mathbb{R}$. We give this only for information, however, as we are concerned primarily with $\eta_1 < 0$, for which a more convenient form is in terms of modified Bessel functions,

$$\eta_2 = \frac{\eta_1}{2}\left(1 - \frac{w}{2}\frac{cK_2(w) + cK_0(w) - I_2(w) - I_0(w)}{cK_1(w) + I_1(w)}\right) \ , \tag{34}$$

re-defining $w = 2\sqrt{-b_1/\eta_1}$. The constant $c \in \mathbb{R}$ can be written as

$$c = \frac{I_2(2\sqrt{b_1}) \ + \ \frac{1+2d}{\sqrt{b_1}}I_1(2\sqrt{b_1}) \ + \ I_0(2\sqrt{b_1})}{K_2(2\sqrt{b_1}) - \frac{1+2d}{\sqrt{b_1}}K_1(2\sqrt{b_1}) + K_0(2\sqrt{b_1})} \ , \tag{35}$$

where d is the value of η_2 when $\eta_1 = -1$. These solutions are plotted in fig. 3(left), and show a set of trajectories exiting the singularity into $\eta_1 < 0$.

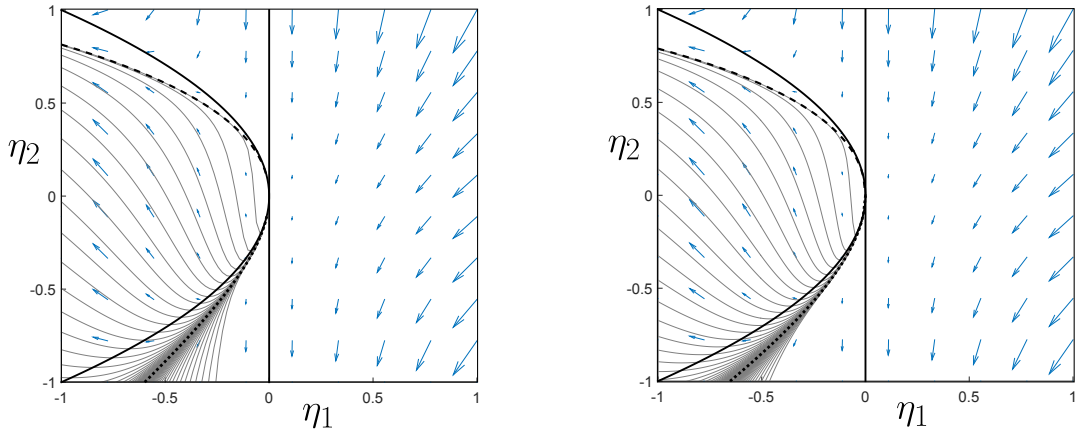

Fig. 3. Plot of the geometry of (30), showing the local flow field, the nullcline of the vertical vector field (thick curve), a number of solutions exiting the origin, and the curves $\eta_{0,\infty}$ bounding those exit solutions (thick dashed curves). Left: exact using (34) and the exact expression from (40); right: asymptotics using (38) and the approximation from (40) neglecting order w^{-2} terms.

For $b_1 = 0$ we recover the solutions of (9). For b_1 non-zero we can approximate the solutions (34) for η_1 close to zero by expanding the Bessel functions for large argument w. The expansions to second order (see e.g. [Abramowitz & Stegun, 1964]) can be collected together concisely as

$$\begin{pmatrix} I_0(w) & K_0(w) \\ I_1(w) & K_1(w) \\ I_2(w) & K_2(w) \end{pmatrix} = \frac{1}{\sqrt{2w}}\begin{pmatrix} 1 & 1/8w \\ 1 & -3/8w \\ 1 & -15/8w \end{pmatrix}\begin{pmatrix} 1 & 1 \\ 1 & -1 \end{pmatrix}\begin{pmatrix} \frac{e^w}{\sqrt{\pi}} & 0 \\ 0 & \frac{\sqrt{\pi}}{e^w} \end{pmatrix} + \mathcal{O}\left(w^{-5/2}\right) \ . \tag{36}$$

Substituting these into (34) and re-arranging we obtain

$$\eta_2 = \frac{2b_1}{w}\frac{c\pi e^{-2w}(1 - \frac{1}{8w}) - (1 + \frac{1}{8w}) + \mathcal{O}\left(w^{-2}\right)}{c\pi e^{-2w}(1 + \frac{3}{8w}) + (1 - \frac{3}{8w}) + \mathcal{O}\left(w^{-2}\right)} \ . \tag{37}$$

This order of approximation is necessary to produce the flow in fig. 3(right), but the behaviour local to the singularity is given by the approximation

$$\begin{aligned}\eta_2 &= -\tfrac{2b_1}{w}\left(1+\tfrac{1}{8w}-2\pi c e^{-2w}\right)+\mathcal{O}\left(w^{-3},e^{-4w},w^{-2}e^{-2w}\right)\\ &= \tfrac{\eta_1}{16}-\sqrt{-b_1\eta_1}\left(1-2\pi c e^{-4/\sqrt{-\eta_1}}\right)+\mathcal{O}\left(\eta_1^{3/2},e^{-8/\sqrt{-\eta_1}},\eta_1 e^{-4/\sqrt{-\eta_1}}\right)\ .\end{aligned} \tag{38}$$

These define a continuum of curves in the (η_1,η_2) plane, such that for every $c\in\mathbb{R}$ there exists a curve passing through the singularity at $(0,0)$.

To find the region of the plane filled by these solutions, observe that in $\eta_1<0$ they have separatrices where $c=0$ and $c\to\infty$, given by

$$\eta_2=\frac{\eta_1}{2}\left(1+\frac{w}{2}\frac{I_2(w)+I_0(w)}{I_1(w)}\right)\ , \tag{39a}$$

$$\eta_2=\frac{\eta_1}{2}\left(1-\frac{w}{2}\frac{K_2(w)+K_0(w)}{K_1(w)}\right)\ , \tag{39b}$$

respectively. Substituting in $w=2\sqrt{-b_1/\eta_1}$ we define these asymptotic expressions as functions $\eta_2^{(0)}(\eta_1)$ and $\eta_2^{(\infty)}(\eta_1)$, respectively. These curves bound a region in which trajectories remain bounded in λ_2 for finite λ_1, from the region outside them where trajectories pass through $\lambda_2\to\pm\infty$ at finite value of λ_1. For large w we have

$$\eta_2^{(0)}(\eta_1)=\frac{2b_1}{-w}\frac{1+\frac{1}{8w}+\mathcal{O}\left(w^{-2}\right)}{1-\frac{3}{8w}+\mathcal{O}\left(w^{-2}\right)}\ ,\qquad w=2\sqrt{-b_1/\eta_1}\ , \tag{40a}$$

$$\eta_2^{(\infty)}(\eta_1)=\frac{2b_1}{w}\frac{1-\frac{1}{8w}+\mathcal{O}\left(w^{-2}\right)}{1+\frac{3}{8w}+\mathcal{O}\left(w^{-2}\right)}\ ,\qquad w=2\sqrt{-b_1/\eta_1}\ . \tag{40b}$$

The exact and asymptotic curves are plotted in fig. 3.

The values of d corresponding to these separatrix values $c=0$ and $c\to\infty$ are some $d=d_-$ and $d=d_+$, respectively, where

$$d_\pm=-\tfrac{1}{2}\pm\frac{\sqrt{b_1}}{2}\frac{K_2(2\sqrt{b_1})+K_0(2\sqrt{b_1})}{K_1(2\sqrt{b_1})}\approx\sqrt{b_1}\frac{1\mp\frac{1}{16\sqrt{b_1}}}{1\pm\frac{3}{16\sqrt{b_1}}}\ . \tag{41}$$

■

The solution curves in fig. 3 illustrate the set of solutions issuing from $\eta_1=\eta_2=0$, generated by varying c.

Note the geometrical interpretation of the constants C and c in the solutions at the codimension 4 and 3 singularities, (11) and (33). In (11) all solutions exit $\eta_1=\eta_2=0$ with the same gradient, $\frac{\mathrm{d}\eta_2}{\mathrm{d}\eta_1}=(1-C\eta_1)^{-2}\to 1$ as $\eta_1\to 0$, and are distinguishable only in their second derivative, $\frac{\mathrm{d}\eta_2}{\mathrm{d}\eta_1}=2C(1-C\eta_1)^{-3}\to 2C$ as $\eta_1\to 0$. In (11) all solutions exit $\eta_1=\eta_2=0$ with the same infinite gradient, in the form of a square root singularity (38), and the constant c relates to the higher order curvature again, though it cannot be extracted directly from the second derivative $\frac{\mathrm{d}^2\eta_2}{\mathrm{d}\eta_1^2}$, but by differentiating instead $(-\eta_1)^{5/2}\eta_2$, giving

$$c=\frac{e^{4\sqrt{-b_1/\eta_1}}}{8\pi\sqrt{b_1}}\frac{d^2}{d\eta_1^2}[(-\eta_1)^{5/2}\eta_2]\ .$$

Similar to (13) in the previous section we may now consider this as part of a slow-fast system

$$\dot{x}_1=v_1+\mathcal{O}\left(\varepsilon\right)\ , \tag{42a}$$

$$\dot{x}_2=v_2+\mathcal{O}\left(\varepsilon\right)\ , \tag{42b}$$

$$\varepsilon\dot{\eta}_1=-x_1-\eta_1^2\ , \tag{42c}$$

$$\varepsilon\dot{\eta}_2=-x_2-b_1\eta_1-\eta_2^2\ . \tag{42d}$$

Solutions are not as easy to obtain as for (13), but the two-timescale (x_1, η_1) subsystem is just the same as in (13), and therefore from lemma 2 and lemma 3 we immediately have the following.

Lemma 5. *A one-parameter family of orbits are attracted in finite time into a neighbourhood of the singularity in* (42) *that is exponentially small in* ε*.*

Lemma 6. *Orbits with initial conditions in an* ε*-neighbourhood of the singularity in the region* $\eta_1, \eta_2 < 0$*, lie an order 1 distance from the singularity after a time* $t = \mathcal{O}\left(\varepsilon^{2/3}\right)$*.*

So as in section 3 we see that exit from an ε-neighbourhood of the singularity occurs in finite time, and in this case fills (approximately) the region $\eta_2 \leq \eta_2^{0,\infty}(\eta_1)$ as defined in lemma 4. The region filled by orbits leaving the singularity is therefore, as seen in fig. 3, larger than that of the more degenerate singularity in fig. 2. Thus the indeterminacy is, perhaps surprisingly, worse in a sense for this less degenerate scenario. The consequences of this are perhaps best illustrated in the original setting where these singularities were found, that of piecewise-smooth dynamical systems.

5. Embedding in a piecewise-smooth system

The singularities studied above arose originally in studying a system of ordinary differential equations with discontinuities along certain thresholds where the quantities η_1, η_2, jump in value, and the systems (13) or (42) arise in resolving dynamics at the discontinuity.

Most generally, consider a system of the form

$$\dot{x}_i = f_i(\mathbf{x}, \mathbf{y}; \lambda_1, \lambda_2) \ , \qquad i = 1, 2, 3, \tag{43a}$$

$$\dot{y}_1 = g_1(\mathbf{x}, \mathbf{y}; \lambda_1, \lambda_2) \ , \tag{43b}$$

$$\dot{y}_2 = g_2(\mathbf{x}, \mathbf{y}; \lambda_1, \lambda_2) \ , \tag{43c}$$

in terms of variables $\mathbf{x} = (x_1, x_2, x_3)$ and $\mathbf{y} = (y_1, y_2)$, and discontinuous quantities known as *switching multipliers* defined as $\lambda_1 = \text{sign}(y_1)$ and $\lambda_2 = \text{sign}(y_2)$. In different applications, switching multipliers are used to model discontinuous physical properties such as Coulomb forces in friction or contact forces in collisions, or switches in electronic, mechanical, or biological control systems.

The equations (43) as stated are not well defined at the discontinuity thresholds $y_1 = 0$ and $y_2 = 0$. The dynamics there can be found by *blowing up* the thresholds, which entails letting $y_i = \varepsilon\lambda_i$ for $|y_i| \leq \varepsilon$ and $|\lambda_i| \leq 1$, for some small parameter $\varepsilon \geq 0$. The interval $\lambda_i \in [-1, +1]$ constitutes the blow up of the infinitesimal interval $y_i \in \varepsilon[-1, +1]$ as $\varepsilon \to 0$.

This blow up of the discontinuities can be performed on each of the thresholds $y_1 = 0$ and $y_2 = 0$ separately. The singularities described above arise at the intersection of these, at $y_1 = y_2 = 0$, where blowing up (43) (i.e. substituting in $y_1 = \varepsilon\lambda_1$ and $y_2 = \varepsilon\lambda_2$ for $\varepsilon \to 0$), gives

$$\dot{x}_i = f_i(\mathbf{x}, \mathbf{0}; \lambda_1, \lambda_2) + \mathcal{O}(\varepsilon) \ , \qquad i = 1, 2, 3, \tag{44a}$$

$$\varepsilon\dot{\lambda}_1 = g_1(\mathbf{x}, \mathbf{0}; \lambda_1, \lambda_2) + \mathcal{O}(\varepsilon) \ , \tag{44b}$$

$$\varepsilon\dot{\lambda}_2 = g_2(\mathbf{x}, \mathbf{0}; \lambda_1, \lambda_2) + \mathcal{O}(\varepsilon) \ . \tag{44c}$$

We have again taken the same small constants ε for the η_1 and η_2 dynamics but could easily take different constants ε_1 and ε_2 if the timescales of switching in λ_1 and λ_2 are not exactly equal.

The dynamics of (44) is studied on the *switching layer*, defined as

$$(x_1, x_2, x_3) \in \mathbb{R}^3 \ , \qquad (\lambda_1, \lambda_2) \in [-1, +1]^2 \ .$$

Let us then assume that there exists a point on this layer, at $(x_1, x_2, x_3) = (0, 0, 0)$ and $(\lambda_1, \lambda_2) = (\lambda_1^*, \lambda_2^*)$, at which lies the singularity defined in (3), using local layer variables

$$\eta_1 = \lambda_1 - \lambda_1^* \ , \qquad \eta_2 = \lambda_2 - \lambda_2^* \ . \tag{45}$$

Then using section 2 we can expand (44) about the origin in $(x_1, x_2, x_3, \eta_1, \eta_2)$ coordinates as

$$\dot{x}_i = f_{i0} + \mathcal{O}\left(\mathbf{x}, \boldsymbol{\eta}, \varepsilon_1, \varepsilon_2\right) \ , \qquad i = 1, 2, 3, \tag{46a}$$

$$\varepsilon\dot{\eta}_1 = a_0(\mathbf{x}, \mathbf{0}) - a_2(\mathbf{x}, \mathbf{0})\eta_2 - \eta_1^2 + \mathcal{O}_1 \ , \tag{46b}$$

$$\varepsilon\dot{\eta}_2 = b_0(\mathbf{x}, \mathbf{0}) - b_1(\mathbf{x}, \mathbf{0})\eta_1 - \eta_2^2 + \mathcal{O}_2 \ , \tag{46c}$$

for some constants f_{i0}, and higher order corrections

$$\left.\begin{aligned} \mathcal{O}_1 &= \mathcal{O}\left(\eta_1^3, \eta_2^2, \eta_1\eta_2^2, x_i\eta_j^2, \varepsilon_1, \varepsilon_2\right) \\ \mathcal{O}_2 &= \mathcal{O}\left(\eta_1^2, \eta_2^3, \eta_1\eta_2^2, x_i\eta_j^2, \varepsilon_1, \varepsilon_2\right) \end{aligned}\right\} \ , \tag{46d}$$

having taken x_i coordinates such that

$$a_0(\mathbf{0}, \mathbf{0}) = b_0(\mathbf{0}, \mathbf{0}) = a_2(\mathbf{0}, \mathbf{0}) = 0 \ . \tag{47}$$

We take three dimensions in $\mathbf{x}$ so that the singularity (3) can occur generically in the overall $n \geq 5$ dimensional system. That is, generically there can exist a point on the intersection of the discontinuity thresholds, $y_1 = y_2 = 0$, at which (47) is satisfied.

5.1. *A mechanical prototype*

To set up a definite example system let us assume that the y_1, y_2, are velocities of mechanical states with displacement x_1, x_2. This is the situation in the original friction problem from [Webber & Jeffrey, 2019], with $y_i = \dot{x}_i - v_i$ describing the velocities of two spring-coupled blocks, relative to the speed v_i of some moving surface on which they have frictional contact. The discontinuity of the Coulomb dry-friction force between each block and the surface is then represented by a switching multiplier $\lambda_j = \text{sign}(y_j)$, and then a local variable $\eta_j = \lambda_j - \lambda_j^*$ is taken about the singularity (3) as described from (43) to (45) above.

Although in [Webber & Jeffrey, 2019] the (y_1, y_2) dynamics was coupled via springs (via dependence on x_i), there was no coupling of the fast η_i dynamics ($a_1 = b_1 = 0$). Let us relax this to allow weak coupling with $b_1 \neq 0$, and include mechanical damping (a y_i dependence in each $\dot{y}_i$ equation). Let x_3 be constant for simplicity. Then we obtain a perturbation of the friction oscillator

$$\dot{x}_i = v_i + y_i \ , \qquad i = 1, 2, \tag{48a}$$

$$\dot{x}_3 = 0 \ , \tag{48b}$$

$$\dot{y}_1 = a_0(\mathbf{x}, \mathbf{y}) - a_2(\mathbf{x}, \mathbf{y})\eta_2 - \eta_1^2 \ , \tag{48c}$$

$$\dot{y}_2 = b_0(\mathbf{x}, \mathbf{y}) - b_1(\mathbf{x}, \mathbf{y})\eta_1 - \eta_2^2 \ , \tag{48d}$$

in terms of switching multipliers $\lambda_1 = \text{sign}(y_1)$, $\lambda_2 = \text{sign}(y_2)$, with coordinates chosen such that

$$a_0(\mathbf{0}, \mathbf{0}) = b_0(\mathbf{0}, \mathbf{0}) = a_2(\mathbf{0}, \mathbf{0}) = 0 \ , \tag{49}$$

with weak frictional coupling via b_1. We can now re-define the x_i coordinates such that

$$a_0(\mathbf{x}, \mathbf{0}) = -x_1 \ , \quad b_0(\mathbf{x}, \mathbf{0}) = -x_2 \ , \quad a_2(\mathbf{x}, \mathbf{0}) = x_3 \ . \tag{50}$$

For simplicity let us assume this does not change the equations (48), and since b_1 does not vanish at the singularity let us take $b_1(x_1, x_2, 0) = b_1$ as a constant, and assume $0 \leq b_1 < 1$ (the case $b_1 < 0$ is similar under a reflection in coordinate axes). Similarly we take $v_i > 0$. For this example we omit any higher order corrections to (48).

The dynamics of (48) is at first glance fairly simple, as intended, and as illustrated in fig. 4. In the vicinity of the singularity we have simply $\dot{y}_1, \dot{y}_2 < 0$ in the slipping modes, that is in $y_1 \neq 0$, $y_2 \neq 0$. Thus, ultimately, any initial conditions with the blocks having positive velocities $y_1 > 0$ or $y_2 > 0$, will eventually lead to negative velocities (relative to the surface on which they sit). As each block changes direction it may experience an episode of sticking on its respective threshold $y_1 = 0$, or $y_2 = 0$.

It is in these sticking modes that the dynamics becomes interesting, in particular when both blocks stick simultaneously, i.e. when solutions pass through $y_1 = y_2 = 0$. Because there are large regions of

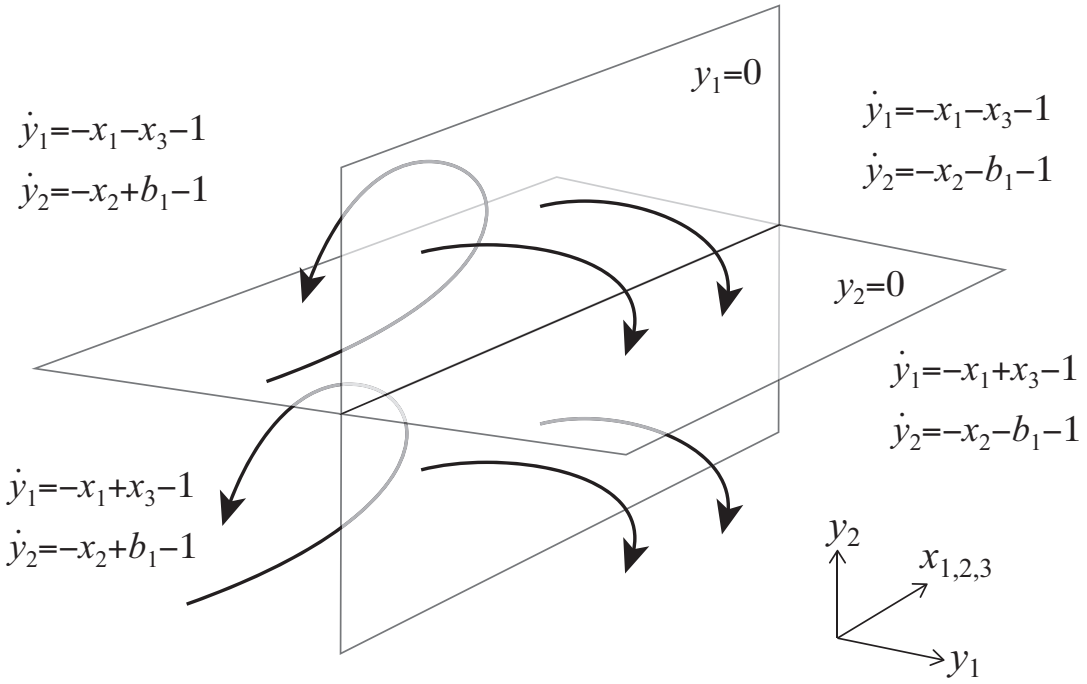

Fig. 4. A representation of the system (48) relative to the sticking thresholds $y_1 = 0$, $y_2 = 0$, (with the x_i coordinates placed along a third 'axis').

$y_1 = y_2 = 0$ for $x_1, x_2, x_3 < 0$ where the righthand of (48) pushes solutions onto $y_1 = 0$ and $y_2 = 0$ in finite time, there exists a large (i.e. non-zero measure) volume of orbits that evolve into this state.

The presence of the singularity in this system then means that trajectories exist that pass through the origin in the sticking state on $y_1 = y_2 = 0$, and then explode into infinitely many possible trajectories as one of the y_js becomes nonzero (i.e. leave the sticking state). For $b_1 = 0$ these immediately then collapse down to an $\mathcal{O}(\varepsilon)$ set of values, so the indeterminacy is fleeting, but for $b_1 \neq 0$ the indeterminacy persists, as the exiting trajectories fill a region of the phase plane in their continued, thereon deterministic, evolution. This is shown as follows.

The state $y_1 = 0$ corresponds to sticking of one block to the surface, the state $y_2 = 0$ to sticking of the other block. Let us first look at the simultaneous sticking state $y_1 = y_2 = 0$.

The switching layer system for (48) on $y_1 = y_2 = 0$ is

$$\dot{x}_i = v_i + \mathcal{O}(\varepsilon) \ , \qquad i = 1, 2, \tag{51a}$$

$$\dot{x}_3 = 0 \ , \tag{51b}$$

$$\varepsilon\dot{\eta}_1 = -x_1 - x_3\eta_2 - \eta_1^2 \ , \tag{51c}$$

$$\varepsilon\dot{\eta}_2 = -x_2 - b_1\eta_1 - \eta_2^2 \ . \tag{51d}$$

The fast (η_1, η_2) subsystem is clearly (42). Lemma 5 therefore tells us that a subset of trajectories in the system evolve into an ε-neighbourhood of the singularity in finite time by tending towards a trajectory

$$(x_1(t), x_2(t), x_3(t), y_1(t), y_2(t)) = \left(v_1 t, v_2 t, 0, \sqrt{-x_1 t}, \sqrt{-v_2 t - b_1\sqrt{-x_1 t}}\right) \ , \tag{52}$$

for $t < 0$, which enters the singularity at time $t = 0$.

Lemma 6 then says these solutions are expelled from the ε-neighbourhood of the singularity in finite time, along the trajectories (34) (or asymptotically (38)) into the region $\eta_2 \leq \eta_2^{0,\infty}(\eta_1)$, which more than fills the quadrant $\eta_1, \eta_2 < 0$ as shown in fig. 3.

These solutions evolve until they reach sufficiently small η_1, η_2, that they leave the layer, i.e. that they leave the sticking mode and slip into $y_1, y_2 < 0$. This happens at $\lambda_1, \lambda_2 = -1$, corresponding to $\eta_1 = -1 - \lambda_1^*$, $\eta_1 = -1 - \lambda_1^*$.

We have then to ask how the two blocks leave the simultaneous sticking state. Which block leaves sticking first depends on which boundary of the layer $(\lambda_1, \lambda_2) \in [-1,+1] \times [-1,+1]$ the solution leaves by.

If a solution reaches $\lambda_2 = -1$ then the first block leaves sticking and evolves into $y_2 < 0$, with the second block still in sticking such that we still have $y_1 = 0$ $\lambda_1 \in [-1,+1]$. To find the dynamics on $y_1 = 0$, specifically on $y_1 = 0 > y_2$ since $\dot{y}_2$ is negative near the singularity, we substitute $y_1 = \varepsilon\lambda_1$ for $\lambda_1 \in [-1,+1]$ into (48), to blow up just the threshold $y_1 = 0$ and so obtain

$$\dot{x}_i = v_i \ , \tag{53a}$$
$$\varepsilon\dot{\eta}_1 = -x_1 - x_3 - \eta_1^2 \ , \tag{53b}$$
$$\dot{y}_2 = -x_2 - b_1\eta_1 - 1 \ . \tag{53c}$$

Since x_i is strictly increasing from $x_i = 0$ at the singularity, we have $x_1, x_2, x_3 > 0$. This implies that $\dot{\eta}_1 < 0$ in (53), so on $y_1 = 0$ there is no sliding, and all trajectories in this region cross the discontinuity threshold from positive to negative y_1. For those solutions exiting the singularity from $y_2 = 0$, they likewise evolve towards $y_1 < 0$. The fastness of the y_2 dynamics collapses these trajectories into an ε-neighbourhood of $y_1 = y_2 = 0$, and hence to

$$(x_1(t), x_2(t), x_3(t), y_1(t), y_2(t)) = \left(v_1 t, v_2 t, 0, -\tfrac{1}{2}v_1 t^2 - t, -\tfrac{1}{2}v_2 t^2 + (b_1 - 1)t\right) + \mathcal{O}\left(\varepsilon^{2/3}\right) \ , \tag{54}$$

in the system on $y_1, y_2 < 0$,

$$\dot{x}_i = v_i \ , \tag{55a}$$
$$\dot{y}_1 = -x_1 - x_3 - 1 \ , \tag{55b}$$
$$\dot{y}_2 = -x_2 + b_1 - 1 \ . \tag{55c}$$

This situation is as described in considerable more depth in [Webber & Jeffrey, 2019] for the uncoupled dry friction oscillator.

If a solution reaches $\lambda_1 = -1$ then something rather different happens, as the weak coupling ensures that the indeterminacy from the singularity persists. The first block leaves sticking and evolves into $y_1 < 0$, with the second block still in sticking such that $\lambda_2 \in [-1,+1]$. Similar to above we must find the dynamics on $y_2 = 0$, specifically on $y_2 = 0 > y_1$ since again $\dot{y}_1$ is negative near the singularity. We substitute $y_2 = \varepsilon\lambda_2$ for $\lambda_2 \in [-1,+1]$ into (48), which blows up the threshold $y_2 = 0$, and we obtain sticking motion of the second block while the first block slips, given by

$$\dot{x}_i = v_i \ , \tag{56a}$$
$$\dot{y}_1 = -x_1 - x_3\eta_2 - 1 \ , \tag{56b}$$
$$\varepsilon\dot{\eta}_2 = -x_2 + b_1 - \eta_2^2 \ . \tag{56c}$$

There is now a sliding mode in this system, given by the set

$$\left\{(\boldsymbol{x}, y_1, \eta_2) \in \mathbb{R}^2 \times [-1,+1] \times \mathbb{R} \ : \ x_2 = b_1 - \eta_2^2\right\} \ , \tag{57}$$

where the second block continues to stick, either along a trajectory

$$(x_1(t), x_2(t), x_3(t), y_1(t), y_2(t)) = \left(v_1 t, v_2 t, v_3 t, -\tfrac{1}{2}v_1 t^2 - t, +\sqrt{b_1 - \tfrac{1}{2}v_2 t}\right) + \mathcal{O}\left(\varepsilon^{2/3}\right) \ , \tag{58}$$

which is attracting, or along a trajectory

$$(x_1(t), x_2(t), x_3(t), y_1(t), y_2(t)) = \left(v_1 t, v_2 t, v_3 t, -\tfrac{1}{2}v_1 t^2 - t, -\sqrt{b_1 - \tfrac{1}{2}v_2 t}\right) + \mathcal{O}\left(\varepsilon^{2/3}\right) \ , \tag{59}$$

which is repelling, with respect to the fast η_2 dynamics. These are depicted in fig. 5.

These particular trajectories collide at a fold of the invariant manifold (57), at $t = 2b_1/v_2$, giving a family of orbits that evolve in time $t = 2b_1/v_2 = \mathcal{O}\left(\varepsilon^{2/3}\right)$ towards the point

$$(x_1(t), x_2(t), x_3(t), y_1(t), y_2(t)) = \tfrac{2b_1}{v_2}\left(v_1, v_2, v_3, -b_1 v_1/v_2 - 1, 0\right) + \mathcal{O}\left(\varepsilon\right) \ . \tag{60}$$

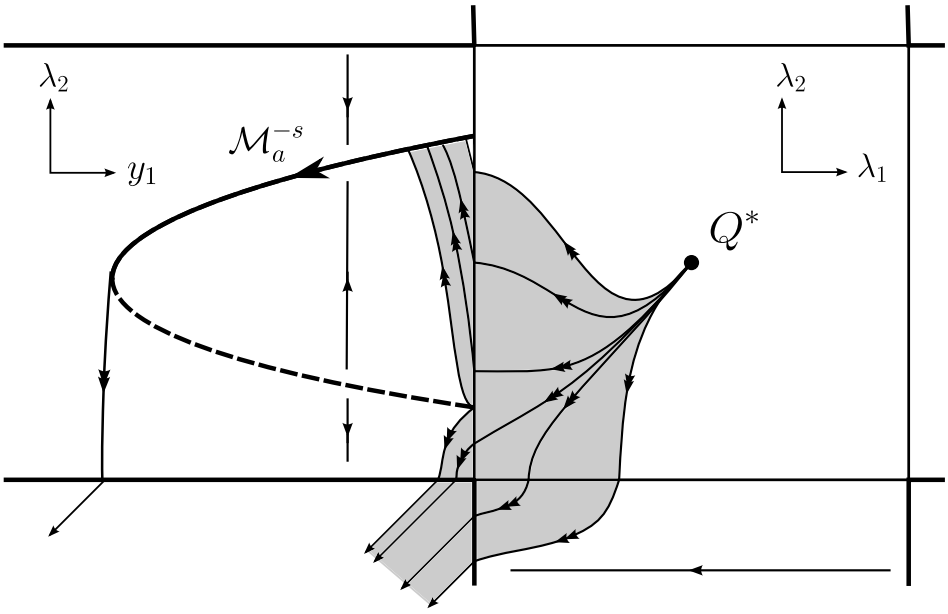

Fig. 5. A sketch of the system (48), schematically tracing out a set-valued solution exiting from the singularity in the layer on $(\lambda_1, \lambda_2) \in [-1, +1]^2$, and entering .

Noting that $\dot{y}_1$ is strictly negative, given that $x_1, x_2, x_3 > 0$ after exit from the singularity, the set of trajectories issuing from the singularity are repelled from (59). They either reach $\lambda_2 = \lambda_2^* + \eta_2(t) = -1$, in which case the second block slips into $y_2 < 0$, or they are attracted towards (58), in which case they evolve to the point (60) before again evolving towards $\lambda_2 = \lambda_2^* + \eta_2(t) = -1$ whereupon the second block slips into $y_2 < 0$. These different solutions now, however, can reach this boundary of the layer either adjacent to the singularity at $y_1 = \mathcal{O}(\varepsilon)$, or in the neighbourhood of the fold (60), and therefore they exit into slip in a range of times $0 \leq t \leq 2b_1/v_2$, over a range of positions

$$0 \leq x_1 \leq \tfrac{2b_1 v_1}{v_2} \ , \qquad 0 \leq x_2 \leq 2b_1 \ , \qquad x_3 = 0 \ , \tag{61}$$

and velocities

$$-\tfrac{2b_1}{v_2}(\tfrac{b_1 v_1}{v_2} + 1) \leq y_1 \leq 0 \ , \qquad y_2 = 0 \ , \tag{62}$$

all correct up to order $\varepsilon^{2/3}$.

Thus in any case, the dynamics ends in the eventual slipping of the blocks in $y_1, y_2 < 0$, but the determinacy breaking at the singularity results in a whole family of trajectories entering the double sticking state at the singularity — merely the familiar state that two oscillating blocks simultaneously stick — followed by evolution into slip that is indeterminable within a substantial range of slipping times, positions, and velocities.

Letting $b_1 \to 0$, the separation between the two distinct exit sets shrinks until forming a single family of exit solutions an order ε apart, corresponding to the codimension 4 singularity as derived from the oscillator, in which a microscopic burst of non-determinism re-collapses on the macroscopic scale.

5.2. *Singular perturbation*

It is natural to ask, when singularities like those above arise in a piecewise-smooth system, whether they persist when the system is smoothed. In the context of mechanics, for example, this corresponds to allowing compliant contact between bodies.

Consider smoothing the discontinuity in η_i by replacing $\eta_i \mapsto -\lambda_i^* + \phi_i(y_i/\varepsilon)$ in (46), where ϕ_i are smoothly (i.e. infinitely) differentiable monotonic functions satisfying

$$\phi_i(y/\varepsilon) = \operatorname{sign}(y) + \mathcal{O}(\varepsilon) \quad \text{if} \quad |y| \geq \varepsilon \ . \tag{63}$$

Substituting these directly into the system (46) on $y_1 = y_2 = 0$, and letting $u_i = y_i/\varepsilon$, gives

$$\dot{x}_i = f_i(\mathbf{x}, \mathbf{0}; \boldsymbol{\eta}) + \mathcal{O}(\varepsilon) \ , \qquad i = 1, 2, 3, \tag{64a}$$

$$\varepsilon \dot{u}_1 = a_0(\mathbf{x}, \mathbf{0}) - a_2(\mathbf{x}, \mathbf{0})[-\lambda_2^* + \phi_2(u_2)] - [-\lambda_1^* + \phi_1(u_1)]^2 + \mathcal{O}_1 \ , \tag{64b}$$

$$\varepsilon \dot{u}_2 = b_0(\mathbf{x}, \mathbf{0}) - b_1(\mathbf{x}, \mathbf{0})[-\lambda_1^* + \phi_1(u_1)] - [-\lambda_2^* + \phi_2(u_2)]^2 + \mathcal{O}_2 \ . \tag{64c}$$

We will assume that $\mathbf{x}$ has been chosen such that (47) holds. This is the equivalent of the layer system (46) but in the smoothing methodology. The error terms, written in terms of η_i still for now, are

$$\left.\begin{aligned} \mathcal{O}_1 &= \mathcal{O}\left(\varepsilon, \eta_1^3, \eta_2^2, \eta_1\eta_2^2, x_i\eta_j^2, \varepsilon_1, \varepsilon_2\right) \\ \mathcal{O}_2 &= \mathcal{O}\left(\varepsilon, \eta_1^2, \eta_2^3, \eta_1\eta_2^2, x_i\eta_j^2, \varepsilon_1, \varepsilon_2\right) \end{aligned}\right\} \ . \tag{65}$$

Define u_i^* such that

$$\phi_i(u_i^*) = \lambda_i^* \ , \tag{66}$$

and let $w_i = u_i - u_i^*$, then expand $\phi_i(u_i) = \phi_i(u_i^*) + w_i\phi_i'(u_i^*) + \frac{1}{2}w_i^2\phi_i''(u_i^*) + ...$ From (64) we then obtain

$$\dot{x}_i = f_i(\mathbf{x}, \mathbf{0}; \boldsymbol{\eta}) + \mathcal{O}(\varepsilon) \ , \qquad i = 1, 2, 3, \tag{67a}$$

$$\varepsilon \dot{w}_1 = a_0(\mathbf{x}, \mathbf{0}) - w_2 a_2(\mathbf{x}, \mathbf{0})\phi_2'(u_2^*) - w_1^2[\phi_1'(u_1^*)]^2 + \mathcal{O}_1 \ , \tag{67b}$$

$$\varepsilon \dot{w}_2 = b_0(\mathbf{x}, \mathbf{0}) - w_1 b_1(\mathbf{x}, \mathbf{0})\phi_1'(u_1^*) - w_2^2[\phi_2'(u_2^*)]^2 + \mathcal{O}_2 \ , \tag{67c}$$

and the error terms become

$$\left.\begin{aligned} \mathcal{O}_1 &= \mathcal{O}\left(\varepsilon, w_1^3, w_2^2, w_1w_2^2, x_iw_j^2, x_iw_2^2\right) \\ \mathcal{O}_2 &= \mathcal{O}\left(\varepsilon, w_1^2, w_2^3, w_1w_2^2, x_iw_j^2, x_iw_1^2\right) \end{aligned}\right\} \ , \tag{68}$$

where $a_2(\mathbf{x}, \mathbf{0})$ and $b_1(\mathbf{x}, \mathbf{0})$ are of order x_i by (49).

Thus the smoothed system (67) exhibits the same local singularity, with a topologically equivalent fast subsystem, to that of the nonsmooth system's layer dynamics (46). Lemma 6 applies directly to (64) by substituting (λ_1, λ_2) with (u_1, u_2): there exists a singularity where $g_1 = g_2 = 0$ and $\frac{\partial g_1}{\partial u_1} = \frac{\partial g_2}{\partial u_2} = \frac{\partial g_1}{\partial u_2} = 0$ (immediately obvious from the local expression (67)), from which the exit is indeterminate — a set-valued flow filling a wide region in $u_1 < 0$.

The proper treatment of this is then by singular perturbation analysis (see e.g. [Fenichel, 1979; Jones, 1995; Sotomayor & Teixeira, 1996] for standard methods). In short, for $\varepsilon \to 0$ this two-timescale system possesses a critical manifold $\mathcal{M}$ where $g_1 = g_2 = 0$, which is equivalent to the sliding manifold $\mathcal{M}$, and for $\varepsilon > 0$ there exist invariant manifolds in the ε-neighbourhood of points where the critical manifold $\mathcal{M}$ is normally hyperbolic with respect the fast (u_1, u_2) subsystem [Jeffrey, 2016, 2019]. Clearly, given the similarity of the righthand sides of (46) and (64), there exists a singularity where (67b)-(67c) vanish, analogous to the singularity in the nonsmooth system.

Typically the study of such singularities under perturbation to $\varepsilon > 0$ is highly non-trivial (see e.g. the singular perturbation of folds of critical manifolds [Wechselberger, 2015] or the regularization of the two-fold singularity in nonsmooth systems [Jeffrey, 2016; eixeira & da Silva, 2012]), due mainly to the lack of explicit expressions for, and potential complexity of, the invariant manifolds for $\varepsilon > 0$.

In this case, however, the situation is rather more simple, as the phenomenon does not depend on the precise form of the invariant manifolds in the ε-neighbourhood of $\mathcal{M}$, but on the existence of the deterministic in-flow, and set-valued out-flow, through the singularity.

6. Closing remarks

The brief study in section 5.1 provides an example of how unpredictability of coupled oscillators can arise due to a local indeterminacy, caused by discontinuity in the defining system, rather than being due to 'complex' global emergence across large number of oscillators.

We looked at the singularity in a five dimensional system to illustrate it with some generality, but five dimensions are not necessarily required to observe the phenomenon, as constraints such as uncoupling may make it generic in lower dimensions. In the mechanical oscillator in [Webber & Jeffrey, 2019] the singularity arose generically in a four dimensional system due to the lack of coupling between the fast subsystems. If the system is continuous in the truncation of (48) then we have

$$\dot{y}_1 = g_1(y_1, y_2) = -\eta_1^2 + \mathcal{O}\left(\eta_1^3, \eta_2^2, y_1, y_2, x_i^2\right) \ , \tag{69a}$$

$$\dot{y}_2 = g_2(y_1, y_2) = -\eta_2^2 + \mathcal{O}\left(\eta_1^2, \eta_2^3, y_1, y_2, x_i^2\right) \ , \tag{69b}$$

and the singularity occurs generically in this planar system in $(y_1, y_2) \in \mathbb{R}^2$, but without any sticking (since there are no x_i coordinates to have sticking motion along), and instead trajectories of the fast subsystem enter and exit the origin in a determinacy-breaking fashion. This appears to be a continuous system, since $\dot{y}_1 = \dot{y}_2 = 1$ for $y_1, y_2 \neq 0$, but discontinuities may still occur through terms of order η_1^3 or η_2^3.

If we relax the '$\gg$' condition in (5) then the size of the set-valued flow through the singularity shrinks, hence the effect of indeterminacy is lessened, until it vanishes when the second derivatives are of similar order, giving a fully deterministic system if we replace the symbol directly in (5) by '$\ll$'.

References

M. Abramowitz and I. Stegun. *Handbook of Mathematical Functions.* Dover, 1964.

V. Acary, H. de Jong, and B. Brogliato. Numerical simulation of piecewise-linear models of gene regulatory networks using complementarity systems. *Physica D*, 269:103–19, 2014.

A. M. Barry, R. McGehee, and E. Widiasih. A Filippov framework for a conceptual climate model. *arXiv:1406.6028*, 2014.

R. Casey, H. de Jong, and J. L. Gouze. Piecewise-linear models of genetic regulatory networks: Equilibria and their stability. *J.Math.Biol.*, 52:27–56, 2006.

E. Davidson and M. Levin. Gene regulatory networks (special feature). *PNAS*, 102(14):4925, 2005.

M. di Bernardo, F. Garofalo, L. Glielmo, and F. Vasca. Switchings, bifurcations, and chaos in dc/dc converters. *IEEE Trans. Circuits Syst. I*, 45:133–141, 1998.

N. Fenichel. Geometric singular perturbation theory. *J. Differ. Equ.*, 31:53–98, 1979.

P. Glendinning, M. R. Jeffrey, & S. Webber. Pausing in piecewise-smooth dynamic systems. *Proc. R. Soc. A*, 475:20180574(1–19), 2019.

N. Hinrichs, M. Oestreich, and K. Popp. On the modelling of friction oscillators. *J. Sound Vib.*, 216(3):435–459, 1998.

M. R. Jeffrey. Hidden degeneracies in piecewise smooth dynamical systems. *Int. J. Bif. Chaos*, 26(5):1650087(1–18), 2016.

M. R. Jeffrey. *Hidden Dynamics: The mathematics of switches, decisions, & other discontinuous behaviour.* Springer, 2019.

H. Jiang, A. S. E. Chong, Y. Ueda, and M. Wiercigroch. Grazing-induced bifurcations in impact oscillators with elastic and rigid constraints. *International Journal of Mechanical Sciences*, 127:204–14, 2017.

C. K. R. T. Jones. *Geometric singular perturbation theory*, volume 1609 of *Lecture Notes in Math. pp. 44-120.* Springer-Verlag (New York), 1995.

G. Karlebach and R. Shamir. Modelling and analysis of gene regulatory networks. *Nature Reviews Molecular Cell Biology*, 9:770–780, 2008.

P. Kowalczyk and P.T. Piiroinen. Two-parameter sliding bifurcations of periodic solutions in a dry-friction oscillator. *Physica D: Nonlinear Phenomena*, 237(8):1053 – 1073, 2008.

J. Leifeld. Nonsmooth homoclinic bifurcation in a conceptual climate model. *arxiv*, pages 1–14, 2016.

E. Plahte and S Kjøglum. Analysis and generic properties of gene regulatory networks with graded response functions. *Physica D*, 201:150–176, 2005.

A. Roberts and P. Glendinning. Canard-like phenomena in piecewise-smooth van der pol systems. *Chaos*, 24(023138):1–11, 2014.

J. Shi, J. Guldner, and V. I. Utkin. *Sliding mode control in electro-mechanical systems.* CRC Press, 1999.

J. Sotomayor and M. A. Teixeira. Regularization of discontinuous vector fields. *Proceedings of the International Conference on Differential Equations, Lisboa*, pages 207–223, 1996.

D. E. Stewart. Rigid-body dynamics with friction and impact. *SIAM Review*, 42(1):3–39, 2000.

W. J. Stronge. *Impact mechanics*. Cambridge University Press, 2004.

M. A. Teixeira and P. R. da Silva. Regularization and singular perturbation techniques for non-smooth systems. *Physica D*, 241(22):1948–55, 2012.

B. Wang, J. Xu, R-J. Wai, and C. Binggang. Adaptive sliding-mode with hysteresis control strategy for simple multimode hybrid energy storage system in electric vehicles. *IEEE Trans. on Industrial Electronics*, 64(2):1404–14, 2017.

S. Webber and M. R. Jeffrey. Micro-slip as a loss of determinacy in dry-friction oscillators. *IJBC*, 29(06):1930015, 2019.

M. Wechselberger. Existence and bifurcation of canards in $\mathbb{R}^3$ in the case of a folded node. *SIAM J. App. Dyn. Sys.*, 4(1):101–139, 2005.

J. Wojewoda, S. Andrzej, M. Wiercigroch, and T. Kapitaniak. Hysteretic effects of dry friction: modelling and experimental studies. *Phil. Trans. R. Soc. A*, 366:747–765, 2008.